J|A|C|S ARTICLES

Published on Web 11/02/2010

Two-Dimensional Polymer Formation on Surfaces: Insight into the Roles of Precursor Mobility and Reactivity

Marco Bieri,*,† Manh-Thuong Nguyen,† Oliver Gröning,† Jinming Cai,† Matthias Treier,†,|| Kamel Aït-Mansour,†,⊥ Pascal Ruffieux,† Carlo A. Pignedoli,† Daniele Passerone,† Marcel Kastler,‡,# Klaus Müllen,‡ and Roman Fasel*,†,§

Empa, Swiss Federal Laboratories for Materials Science and Technology, Feuerwerkerstrasse 39, CH-3602 Thun, and Ueberlandstrasse 129, CH-8600 Duebendorf, Switzerland, Max Planck Institute for Polymer Research, Ackermannweg 10, D-55128 Mainz, Germany, and Department of Chemistry and Biochemistry, University of Bern, Freiestrasse 3, CH-3012 Bern, Switzerland

Received September 3, 2010; E-mail: marco.bieri@empa.ch

Abstract: We report on a combined scanning tunneling microscopy (STM), X-ray photoelectron spectroscopy (XPS), and density functional theory (DFT) study on the surface-assisted assembly of the hexaiodo-substituted macrocycle cyclohexa-*m*-phenylene (CHP) toward covalently bonded polyphenylene networks on Cu(111), Au(111), and Ag(111) surfaces. STM and XPS indicate room temperature dehalogenation of CHP on either surface, leading to surface-stabilized CHP radicals (CHPRs) and coadsorbed iodine. Subsequent covalent intermolecular bond formation between CHPRs is thermally activated and is found to proceed at different temperatures on the three coinage metals. The resulting polyphenylene networks differ significantly in morphology on the three substrates: On Cu, the networks are dominated by "open" branched structures, on the Au surface a mixture of branched and small domains of compact network clusters are observed, and highly ordered and dense polyphenylene networks form on the Ag surface. Ab initio DFT calculations allow one to elucidate the diffusion and coupling mechanisms of CHPRs on the Cu(111) and Ag(111) surfaces. On Cu, the energy barrier for diffusion is significantly higher than the one for covalent intermolecular bond formation, whereas on Ag the reverse relation holds. By using a Monte Carlo simulation, we show that different balances between diffusion and intermolecular coupling determine the observed branched and compact polyphenylene networks on the Cu and Ag surface, respectively, demonstrating that the choice of the substrate plays a crucial role in the formation of two-dimensional polymers.

Introduction

Supramolecular structures formed by the surface-confined self-assembly of functional molecular building blocks are a promising class of materials for future technologies.[1−3] Particularly efficient for their fabrication is hydrogen bonding, which provides both high selectivity and directionality: highly ordered hydrogen-bonded porous molecular networks have been fabricated on well-defined surfaces under ultrahigh vacuum (UHV) conditions.[4−6] Other promising strategies for the self-organized growth of regular supramolecular structures rely on surface metal coordination[7−9] or aromatic coupling motifs.[10] However, a common feature of these nanostructures is, due to the comparably weak interaction energies, the poor thermal and chemical stability that limits their use in potential applications. The obvious requirement for more stable structures has recently led to great interest in covalently bonded two-dimensional molecular networks.[11,12] Various proof-of-principle studies have demonstrated that different reactions readily proceed on surfaces, even though the reactants are confined to two dimensions (2D).[13−22] However, despite the recent progress, the self-

† Swiss Federal Laboratories for Materials Science and Technology.
‡ Max Planck Institute for Polymer Research.
§ University of Bern.
|| Present address: Institut de Science et d'Ingénierie Supramoléculaires (I.S.I.S.), Université de Strasbourg 8, Allée Gaspard Monge, Strasbourg 67000, France.
⊥ Present address: Institute of Condensed Matter Physics, Ecole Polytechnique Fédérale de Lausanne (EPFL), CH-1015 Lausanne, Switzerland.
Present address: BASF SE, GKS/E-B001, D-67056 Ludwigshafen, Germany.

(1) Whitesides, G. M.; Mathias, J. P.; Seto, C. T. *Science* **1991**, *254*, 1312–1319.
(2) Lindsey, J. S. *New J. Chem.* **1991**, *15*, 153–180.
(3) Philp, D.; Stoddart, J. F. *Angew. Chem., Int. Ed. Engl.* **1996**, *35*, 1155–1196.
(4) Theobald, J. A.; Oxtoby, N. S.; Phillips, M. A.; Champness, N. R.; Beton, P. H. *Nature* **2003**, *424*, 1029–1031.
(5) Barth, J. V.; Costantini, G.; Kern, K. *Nature* **2005**, *437*, 671–679.
(6) Barth, J. V. *Annu. Rev. Phys. Chem.* **2007**, *58*, 375–407.
(7) Stepanow, S.; Lingenfelder, M.; Dmitriev, A.; Spillmann, H.; Delvigne, E.; Lin, N.; Deng, X. B.; Cai, C. Z.; Barth, J. V.; Kern, K. *Nat. Mater.* **2004**, *3*, 229–233.
(8) Schickum, U.; Decker, R.; Klappenberger, F.; Zoppellaro, G.; Klyatskaya, S.; Ruben, M.; Silanes, I.; Arnau, A.; Kern, K.; Brune, H.; Barth, J. V. *Nano Lett.* **2007**, *7*, 3813–3817.
(9) Barth, J. V. *Surf. Sci.* **2009**, *603*, 1533–1541.
(10) Treier, M.; Ruffieux, P.; Groning, P.; Xiao, S. X.; Nuckolls, C.; Fasel, R. *Chem. Commun.* **2008**, 4555–4557.
(11) Gourdon, A. *Angew. Chem., Int. Ed.* **2008**, *47*, 6950–6953.
(12) Perepichka, D. F.; Rosei, F. *Science* **2009**, *323*, 216–217.
(13) Grill, L.; Dyer, M.; Lafferentz, L.; Persson, M.; Peters, M. V.; Hecht, S. *Nat. Nanotechnol.* **2007**, *2*, 687–691.
(14) Matena, M.; Riehm, T.; Stohr, M.; Jung, T. A.; Gade, L. H. *Angew. Chem., Int. Ed.* **2008**, *47*, 2414–2417.

organized growth toward extended and regular 2D covalent networks still defines one of the major challenges in surface chemistry.[23]

A partial explanation for this situation is related to the fact that the formation of covalent intermolecular bonds, in contrast to noncovalent bonding, is usually an irreversible process; therefore, molecules confined to covalent structures on surfaces are firmly anchored, and postcorrection of defects or modification of morphology is usually not possible. Thus, to minimize defects in covalent networks and to steer the on-surface synthesis toward desired structures, a detailed understanding of the influence of adsorption energies, diffusion barriers, and lateral interactions of molecular precursors, all of which depend on the substrate atomic environment, symmetry, and chemical nature, is required. Up to the present day, however, there exists little experimental and computational insight into the role of the substrate in on-surface chemical routes toward two-dimensional covalent networks.

Here, we present a combined experimental and computational study of the impact of the substrate on the formation and connectivity of a two-dimensional polymer. We use a prototypical multidentate molecular precursor, the hexaiodo-substituted macrocycle cyclohexa-*m*-phenylene (CHP) (Figure 1),[24] and exploit covalent intermolecular bond formation on the coinage metal surfaces Cu(111), Au(111), and Ag(111). On either surface, the adsorption of CHP at RT results in C−I bond cleavage, giving rise to the formation of surface-stabilized CHP radicals (CHPRs) and coadsorbed iodine. Thermally activated CHPR addition is found to proceed at different temperatures on the three metals, notably at about 475 K (Cu), 525 K (Au), and 575 K (Ag). The morphology of the resulting polyphenylene networks differs significantly: On Cu, the growth of dendritic network structures with single-molecule-wide branches prevails; the Au surface promotes the evolution of small 2D network domains, and on the Ag surface extended and well-ordered 2D networks emerge as we have reported recently.[25,26] With the aid of density functional theory (DFT) calculations, the nature of the surface-stabilized CHPRs, as well as the details of diffusion and reaction pathways, are elucidated. We find that on Cu, diffusion of CHPR is hindered, while the coupling step is significantly promoted. On Ag, on the other hand, the CHPRs retain a high surface mobility but exhibit a low coupling affinity. We demonstrate that these differences are responsible for the formation of dendritic and 2D polyphenylene networks as observed on Cu and Ag surfaces, respectively.

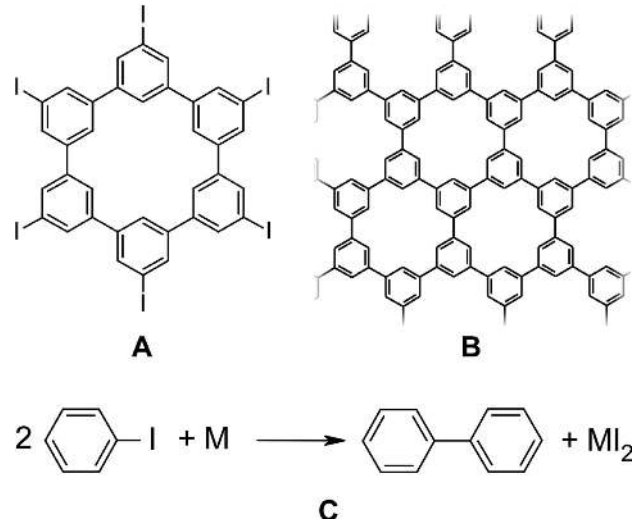

Figure 1. (A) Chemical structure of hexaiodo-substituted CHP. (B) Chemical structure of a fraction of the polyphenylene network. (C) Mechanism of the surface-assisted aryl−aryl coupling of iodobenzene to biphenyl (here, M represents Cu, Au, or Ag).

Results and Discussion

Adsorption of CHP on Cu(111), Au(111), and Ag(111): Evolution of Surface-Stabilized Radicals and Coadsorbed Iodine. Figure 2A shows an overview STM image of CHP molecules adsorbed on Cu(111) that was held at room temperature during deposition (see the Supporting Information for experimental details). CHP agglomerates to small islands of a few molecules, which are distributed over the terraces. Individual molecules can only be spotted along the step edge. Figure 2B shows a high-resolution STM image of two CHPs overlaid with the optimized structure of the molecule derived from DFT calculations (drawn to scale). Line profile analysis across the molecules yields a center-to-center distance of about 1.6 nm, which indicates that the CHPs are not covalently bonded under the applied experimental conditions. Around the CHPs, bright spherical features can be discerned, which are distributed evenly around the molecules. The distance between these features is about 1.8 nm, which is significantly more than the value of the distance between two diametrally opposite CHP iodine atoms (1.5 nm). Furthermore, careful inspection of Figure 2A shows that not all molecules are surrounded by such features and that some of the latter are "shared" by multiple molecules (see, e.g., the three islands marked by white circles). The position as well as the distribution of the spherical features thus suggest C−I bond cleavage upon adsorption of CHP on Cu(111) at room temperature.

To confirm this conclusion, XPS experiments were performed. Figure 2C shows XPS spectra of the I 3d core levels. The red trace refers to the spectrum that was recorded after depositing a submonolayer of CHP on Cu(111) at room temperature. The spectrum reveals two narrow peaks at 630.6 and 619.1 eV binding energy, which correspond to the I $3d_{3/2}$ and I $3d_{5/2}$ spin−orbit split levels. The reference spectrum represented by the green trace corresponds to Cu−I, which was obtained after depositing a submonolayer of iodine on Cu(111) at room

(15) Zwaneveld, N. A. A.; Pawlak, R.; Abel, M.; Catalin, D.; Gigmes, D.; Bertin, D.; Porte, L. *J. Am. Chem. Soc.* **2008**, *130*, 6678–6679.
(16) Weigelt, S.; Busse, C.; Bombis, C.; Knudsen, M. M.; Gothelf, K. V.; Laegsgaard, E.; Besenbacher, F.; Linderoth, T. R. *Angew. Chem., Int. Ed.* **2008**, *47*, 4406–4410.
(17) Veld, M. I.; Iavicoli, P.; Haq, S.; Amabilino, D. B.; Raval, R. *Chem. Commun.* **2008**, 1536–1538.
(18) Treier, M.; Richardson, N. V.; Fasel, R. *J. Am. Chem. Soc.* **2008**, *130*, 14054–14055.
(19) Lipton-Duffin, J. A.; Ivasenko, O.; Perepichka, D. F.; Rosei, F. *Small* **2009**, *5*, 592–597.
(20) Gutzler, R.; Walch, H.; Eder, G.; Kloft, S.; Heckl, W. M.; Lackinger, M. *Chem. Commun.* **2009**, 4456–4458.
(21) Schmitz, C. H.; Ikonomov, J.; Sokolowski, M. *J. Phys. Chem. C* **2009**, *113*, 11984–11987.
(22) Kanuru, V. K.; Kyriakou, G.; Beaumont, S. K.; Papageorgiou, A. C.; Watson, D. J.; Lambert, R. M. *J. Am. Chem. Soc.* **2010**, *132*, 8081–8086.
(23) Sakamoto, J.; van Heijst, J.; Lukin, O.; Schluter, A. D. *Angew. Chem., Int. Ed.* **2009**, *48*, 1030–1069.
(24) Pisula, W.; Kastler, M.; Yang, C.; Enkelmann, V.; Mullen, K. *Chem.—Asian J.* **2007**, *2*, 51–56.
(25) Bieri, M.; Treier, M.; Cai, J.; Ait-Mansour, K.; Ruffieux, P.; Groning, O.; Groning, P.; Kastler, M.; Rieger, R.; Feng, X.; Mullen, K.; Fasel, R. *Chem. Commun.* **2009**, 6919–6921.
(26) Blankenburg, S.; Bieri, M.; Fasel, R.; Mullen, K.; Pignedoli, C. A.; Passerone, D. *Small* **2010**, *6*, 2266–2271.

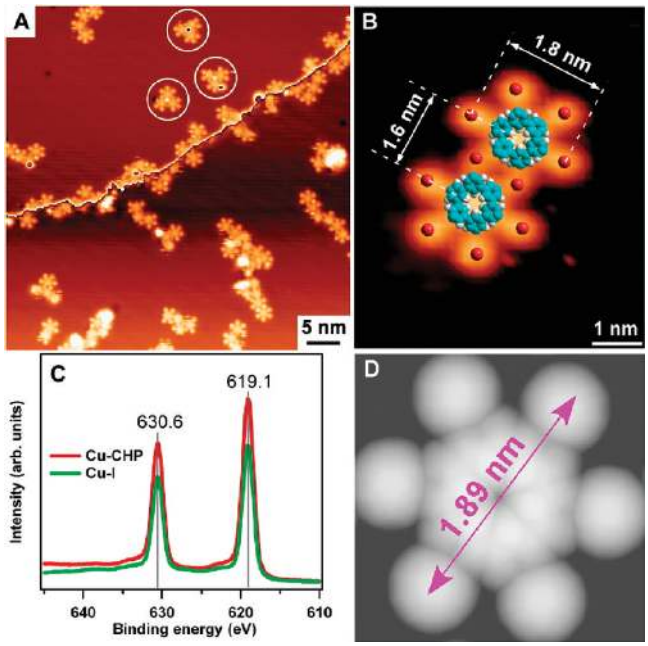

Figure 2. (A) STM image[43] (−2 V, 20 pA) of CHP adsorbed on Cu(111) held at room temperature. Full color contrast has been applied individually to both terraces visible in the image. (B) STM image (−2 V, 20 pA) of two CHP molecules on Cu(111). A model of the molecule is overlaid and drawn to scale. Detached iodine atoms that assemble around the surface-stabilized CHP radicals are indicated as red spheres. (C) XPS spectra of the I 3d core level. The red trace refers to a spectrum that was recorded after depositing a submonolayer of CHP on Cu(111). The green trace was obtained after adsorbing a submonolayer of iodine on Cu(111). Both spectra were recorded at room temperature. (D) STM simulation[44] of a molecule radical encircled by coadsorbed iodine atoms on Cu(111).

temperature. As is obvious, both spectra are in excellent agreement, and no shifts of the core level peaks are detectable, which indicates the presence of Cu−I (and the absence of C−I) species after adsorbing CHP on Cu(111). Furthermore, the peak position of I $3d_{5/2}$ at 619.1 eV agrees well with previous studies for Cu−I compounds.[19,27−29] Peak shifts between Cu−I and Cu−CHP were not observed for the I 4d and I 4s core levels (data not shown). Our conclusion on C−I bond scission is further supported by XPS investigations by Zhou and White on the thermal decomposition of C_2H_5I on Ag(111).[30] In this study, it was shown that the dissociation of the C−I bond is manifested by a significant shift of the I $3d_{5/2}$ peak to lower binding energies, indicating that metal−I and C−I species are readily distinguishable in XPS spectra. On the basis of the STM and XPS results, we thus conclude that the CHP molecule readily dehalogenates upon adsorption on Cu(111), leaving surface-stabilized CHP radicals (CHPRs) and coadsorbed iodine on the surface. The evolution of CHPRs was also observed on Au(111) and Ag(111) at room temperature (data not shown). These findings are in agreement with previous studies reporting on the dissociative adsorption of small alkyl or aryl halides on metal surfaces.[31] Specifically, the C−I bond in iodobenzene, which can be regarded as a subunit of CHP, has been reported to dissociate below room temperature on Cu(111),[32−34] Au(111),[35] and Ag(111),[36] resulting in adsorbed phenyl and iodine.

The notion "surface-stabilized radical" requires some further explanation. Because of their unpaired electrons, radicals are usually associated with high chemical reactivity and short lifetime. However, this picture does obviously not hold for radicals adsorbed on a metal surface under UHV conditions. In this case, the free electrons of the metal surface readily couple to the unpaired electrons of the radical. Plots of the calculated charge density for CHPR located in energetically favorable on-top configurations confirm that the radical strongly binds via six covalent bonds to both the Cu(111) and the Ag(111) surface atomic lattices. The corresponding projected density of states (PDOS) diagrams, shown in Figure S3 of the Supporting Information, confirm a modification of the d electronic band for the involved metal atoms due to the bonding to the dehalogenated carbon atoms. Strictly speaking, the term "radical" is thus not quite correct, but for simplicity we use this terminology to refer to the dehalogenated, surface-stabilized CHP species. STM delivers further experimental evidence for a strong surface interaction: The CHPR species is easily imaged at room temperature even at very low surface coverage (Figure 2A), whereas the structurally similar polyaromatic hydrocarbon hexa-*peri*-hexabenzocoronene (HBC) is highly mobile under similar experimental conditions.[37] In fact, calculated adsorption energies are −15 eV for CHPR/Cu(111) and −11 eV for CHPR/Ag(111) (see the Supporting Information for discussion and analysis of various adsorption geometries for CHPR on Cu and Ag). We note that the adsorption energy is calculated as the energy difference between the most stable atop orientation of the radical on the metal surface and the total energy of the two individual systems, that is, the surface-mimicking slab and CHPR held in the middle of the vacuum region. The considerable energy of adsorption is thus related to the high energy of the radical in vacuum.

So far, it has been implied that the bright spherical features around CHPR refer to iodine atoms. However, in earlier work by Xi and Bent, these authors proposed two different potential bonding geometries for phenyl on Cu(111), notably a phenyl-induced elevation of a surface metal atom to achieve both σ- and π-interactions, and flat-laying phenyl groups bound as anions.[32] On the other hand, the preferential allocation of halogens around surface-stabilized radicals has been observed for diiodobenzene on Cu(110).[19] From our DFT calculations (see the Supporting Information), we find that the observed structures in the STM images (Figure 2B) are in excellent agreement with iodine occupying hollow sites adjacent to CHPR, as is evident by inspecting the STM simulation in Figure 2D. Furthermore, the calculated iodine−iodine distance (1.89 nm) agrees very well with observation (1.8 nm). In contrast, assuming Cu adatoms binding to CHPR, DFT predicts a distance of only 1.54 nm, which is significantly shorter than the experimental value (Supporting Information, Figure S1).

(27) Kovacs, I.; Solymosi, F. *J. Phys. Chem. B* **1997**, *101*, 5397–5404.
(28) Carley, A. F.; Coughlin, M.; Davies, P. R.; Morgan, D. J.; Roberts, M. W. *Surf. Sci.* **2004**, *555*, L138–L142.
(29) Bushell, J.; Carley, A. F.; Coughlin, M.; Davies, P. R.; Edwards, D.; Morgan, D. J.; Parsons, M. *J. Phys. Chem. B* **2005**, *109*, 9556–9566.
(30) Zhou, X. L.; White, J. M. *Catal. Lett.* **1989**, *2*, 375–384.
(31) Bent, B. E. *Chem. Rev.* **1996**, *96*, 1361–1390.
(32) Xi, M.; Bent, B. E. *Surf. Sci.* **1992**, *278*, 19–32.
(33) Xi, M.; Bent, B. E. *J. Am. Chem. Soc.* **1993**, *115*, 7426–7433.
(34) Yang, M. X.; Xi, M.; Yuan, H. J.; Bent, B. E.; Stevens, P.; White, J. M. *Surf. Sci.* **1995**, *341*, 9–18.
(35) Syomin, D.; Koel, B. E. *Surf. Sci.* **2001**, *490*, 265–273.
(36) Szulczewski, G. J.; White, J. M. *Surf. Sci.* **1998**, *399*, 305–315.
(37) Ruffieux, P.; Groning, O.; Fasel, R.; Kastler, M.; Wasserfallen, D.; Mullen, K.; Groning, P. *J. Phys. Chem. B* **2006**, *110*, 11253–11258.

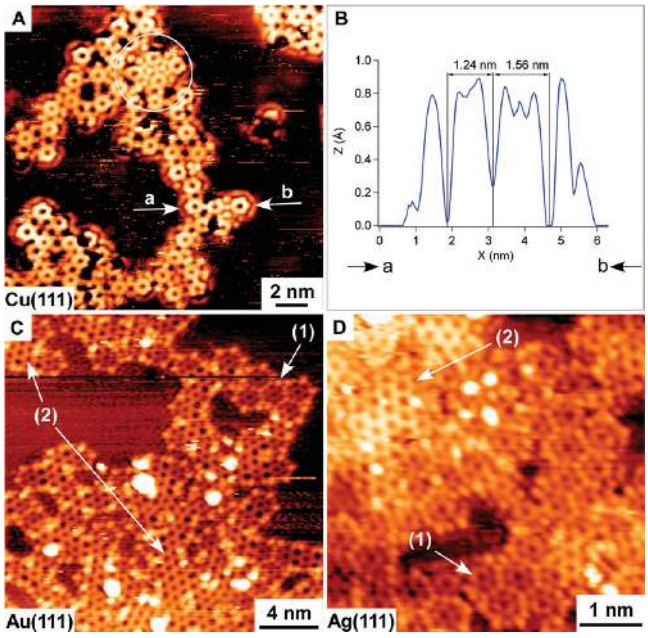

Figure 3. Set of STM images showing the onset of the thermally activated CHP radical addition reaction on the coin metal surfaces Cu(111) (A,B), Au(111) (C), and Ag(111) (D). (A) STM image (−1 V, 200 pA) recorded after CHP deposition on Cu(111) held at RT and postannealing the sample at 475 K for 5 min. The white circle highlights radicals surrounded by iodine atoms. (B) Line profile along arrows a,b shown in (A) with the black vertical lines denoting the center of the CHP species. (C) STM image (−0.8 V, 20 pA) recorded after CHP deposition on Au(111) held at room temperature and postannealing the sample at 525 K for 5 min. (D) STM image (−1.5 V, 30 pA) recorded after CHP deposition on Ag(111) held at room temperature and postannealing the surface at 575 K for 5 min. In (C,D), arrows (1) point to areas of unreacted molecules, and arrows (2) mark covalently interlinked species.

From Surface-Stabilized CHP Radicals to Covalently Bonded Polyphenylene Networks. The STM, XPS, and DFT results discussed in the previous section clearly demonstrate dissociative adsorption of CHP on Cu, Au, and Ag. The subsequent formation of covalently bonded networks is based on thermally activated aryl−aryl homocoupling (see scheme in Figure 1C). The STM images in Figure 3 summarize the experimental findings, which give strong evidence for covalent intermolecular bond formation. Figure 3A shows coupled and uncoupled CHP species as well as iodine atoms on the Cu(111) surface. A prominent domain of uncoupled radicals surrounded by iodine atoms is highlighted in the image (white circle). A line profile analysis (Figure 3B) of adjacent species reveals CHP−CHP distances of 1.24 and 1.56 nm. The former value is in excellent agreement with DFT calculations of covalently bonded molecules, whereas the latter clearly indicates uncoupled radicals (e.g., shown in Figure 2B). Figure 3C and D displays the evolution of covalently bonded species on Au and Ag, respectively. Prominent domains of iodine-surrounded radicals and domains of polymerized radicals are highlighted by arrows (1) and (2). The observed CHPR polymerization is consistent with previous reports on iodobenzene coupling on Cu(111),[32,33] Au(111),[35] and Ag(111).[38,39] However, we find significantly different annealing temperatures to initiate intermolecular bonding on the three coinage metal surfaces, notably Cu (∼475 K) < Au (∼525 K) < Ag (∼575 K), which implies that the nature of the surface plays an important role in intermolecular coupling.

Figure 4 shows STM images of fully polymerized polyphenylene networks supported on Cu(111), Au(111), and Ag(111). Below each overview image, the structures are resolved in more detail. The network morphologies differ significantly on the three substrates. On Cu(111) (Figure 4A,B), branched low-density clusters with single-molecule-wide branches prevail. Careful inspection further reveals the presence of iodine atoms along the border of the structures (Figure 4B, experimental condition: 5 min postannealing step at 675 K). On the other hand, on Au(111) the homocoupling of CHP leads to a mixture of branched and denser polyphenylene clusters as can be identified in Figure 4C,D. No iodine is discerned because the polymerization was performed during a 5 min postannealing step at 745 K. Figure 4E,F eventually shows that dense and highly ordered networks extend on the silver surface. No residual iodine can be identified after performing the polymerization at 825 K for 5 min (Figure 4F).

Monte Carlo Simulations of Covalent Network Growth. To better understand the origin of the significantly different network morphologies, we used a generic Monte Carlo process to simulate the diffusion and assembly of molecules on a hexagonal surface lattice (see the Supporting Information for a detailed model description). Briefly, a seed molecule fixed to the center of the lattice serves as nucleation site, and the subsequent growth of network clusters is based on iterative addition of molecules. The molecules are free to perform a random walk on the simulation grid; when they reach a possible binding site, their affinity to join the seed or a cluster is given by the coupling probability P, which can be interpreted as the ratio between the reaction rate of the coupling step and the total number of events, that is, coupling and diffusion, according to

$$P = \frac{\nu_{\mathrm{coupl}}}{\nu_{\mathrm{coupl}} + \nu_{\mathrm{diff}}} \text{ with } 0 \le P \le 1 \qquad (1)$$

where ν_{coupl} and ν_{diff} denote the reaction rates for the coupling and diffusion steps, respectively. Very high or low coupling probabilities readily allow the following inference on the reaction rates for coupling and diffusion:

$$P \approx 1, \text{ if } \nu_{\mathrm{coupl}} \gg \nu_{\mathrm{diff}}, \text{ and } P \approx 0, \text{ if } \nu_{\mathrm{diff}} \gg \nu_{\mathrm{coupl}} \qquad (2)$$

Figure 5 displays simulated network clusters of 400 molecules by using coupling probabilities $P = 1$, 0.1, and 0.01, respectively. For a more quantitative description, a histogram showing the coordination number distribution of the molecules is appended below each cluster. In the growth regime corresponding to $P = 1$, a diffusing molecule immediately sticks to the cluster when and where it hits the cluster. Note that this condition is equivalent to the classical diffusion-limited aggregation (DLA) model[40] that was applied to study metal−particle aggregation processes. As a consequence, characteristic branched "fractal-like" polyphenylene network structures with single-molecule-wide branches develop (Figure 5A). By lowering the coupling probability by 1 order of magnitude, the evolution of denser network domains can be discerned (Figure 5B). Eventually, compact network formation occurs for $P = 0.01$ (Figure 5C). Thus, by gradually increasing ν_{diff} and reducing ν_{coupl}, denser network clusters emerge. This can readily be understood

(38) Zhou, X. L.; Castro, M. E.; White, J. M. *Surf. Sci.* **1990**, *238*, 215–225.
(39) Zhou, X. I.; Schwaner, A. L.; White, J. M. *J. Am. Chem. Soc.* **1993**, *115*, 4309–4317.
(40) Witten, T. A.; Sander, L. M. *Phys. Rev. Lett.* **1981**, *47*, 1400–1403.

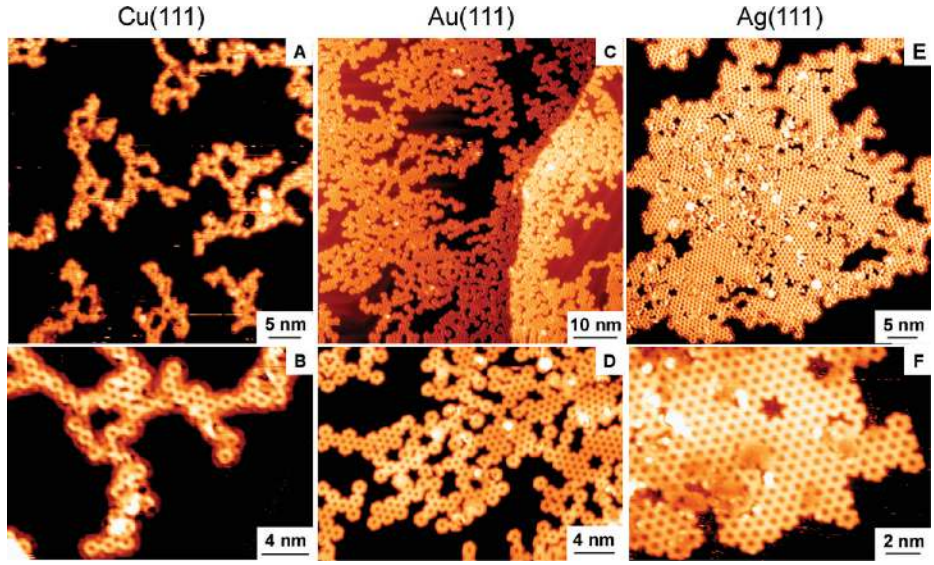

Figure 4. Top panels: Overview STM images of polyphenylene networks on Cu(111), Au(111), and Ag(111). Bottom panels: High-resolution STM images of the polyphenylene networks shown above. Tunneling parameters are (−2 V, 20 pA) (A), (1.5 V, 300 pA) (B), (−1 V, 50 pA) (C), (−1 V, 50 pA) (D), (−0.8 V, 50 pA) (E), and (−1 V, 50 pA) (F). STM topographs shown in panels (E) and (F) are related to the images reported in ref 25.

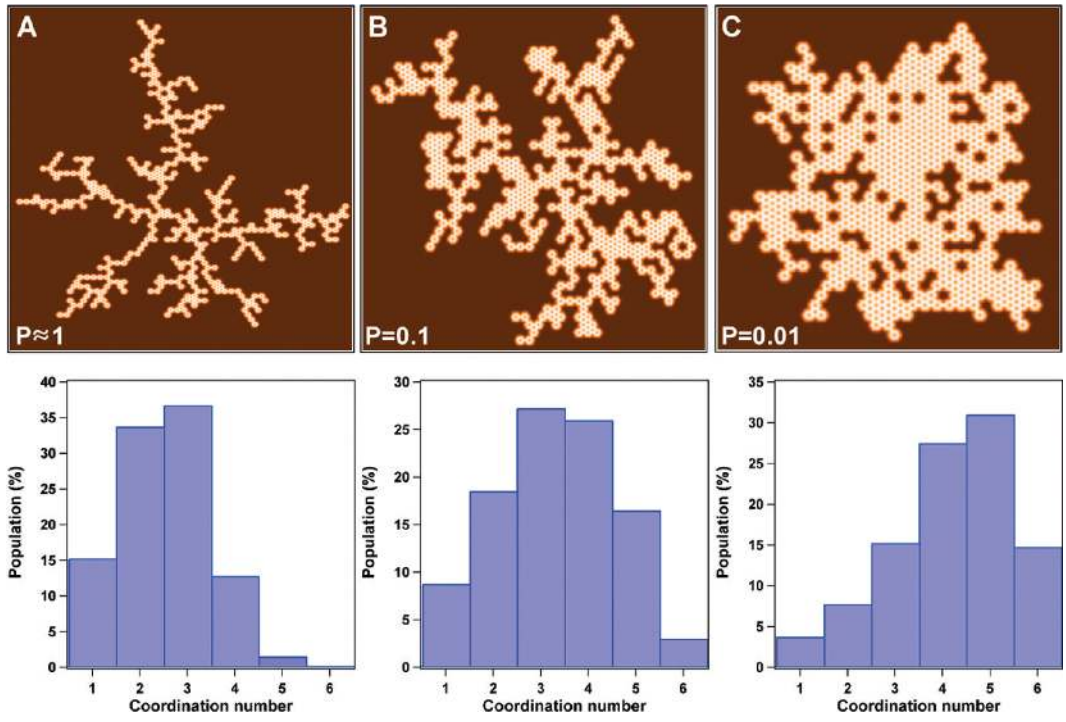

Figure 5. Monte Carlo simulations of molecular network growth. For the networks shown in panels A−C, coupling probabilities of $P = 1$, 0.1, and 0.01, respectively, were used for the growth of clusters consisting of 400 molecules. Below each simulation, the corresponding coordination number distribution of the molecules in the cluster is given.

with simple reasoning: To promote the formation of compact structures, molecules must diffuse along the borders of islands and eventually occupy higher coordinated sites, a process that requires a high mobility and/or low coupling affinity of the reactants. However, it is equally important to notice that even under favorable growth conditions, defects discernible as "holes" in the clusters (Figure 5B,C) occur. These defects arise when six CHP units join at their meta positions to a circle. Because molecules are not allowed to cross over island borders, these defects persist in the clusters. These theoretical findings are in excellent agreement with experiment; "holes" with a characteristic star-shape pattern can easily be spotted within domains of the polyphenylene networks grown on Au(111) and Ag(111) (Figure 4D, F). More importantly, the sequence of the presented cluster simulations is in excellent agreement with the polyphenylene networks grown on Cu(111), Au(111), and Ag(111) (compare Figures 4 and 5), which clearly points to different growth regimes for the covalent assembly of CHP on these surfaces.

DFT Calculations on CHPR Diffusion and Reaction Pathways on Cu(111) and Ag(111). To gain deeper insight into the energetics of the surface-confined polymerization of CHP, we performed extensive ab inito DFT calculations. We focused on CHP/Cu(111) and CHP/Ag(111) because the assembled

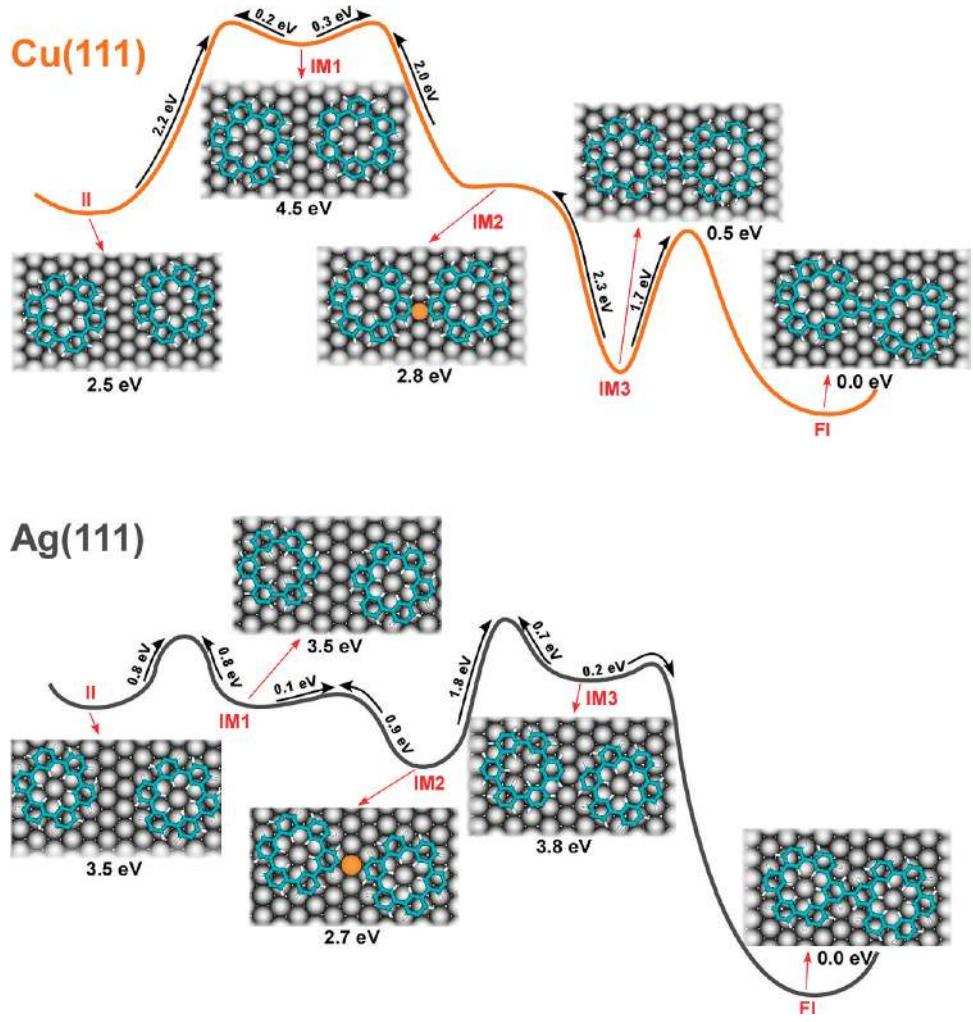

Figure 6. Energy diagrams of the reaction pathways for CHPR−CHPR coupling on Cu(111) (top) and Ag(111) (bottom) elucidated via NEB calculations. Pictorial representations (top views) of the molecule−surface configuration are given for the initial (II), intermediate (IM), and final (FI) states, respectively. The energies below each configuration are given with respect to the total energy of the final state. On both surfaces, the orange sphere indicates the central metal atom bonded to both CHPRs prior to intermolecular bond formation.

polymer networks are found to differ most significantly in structure and morphology on these two substrates. In a first step, the diffusion pathway of a "free", single CHPR on the Cu(111) and Ag(111) surface lattices is investigated via nudged elastic band (NEB) calculations (a detailed discussion of the calculation methods is provided in the Supporting Information). We find that on both substrates the molecule performs a rotational movement (see Supporting Information, Figure S4) between energetically favorable atop positions and that the corresponding diffusion barrier is higher on Cu(111) (2.2 eV) than on Ag(111) (0.8 eV). The difference in the diffusion barrier is related to the strength of the metal−CHPR bond, which is consistent with the reported higher chemical activity of Cu(111) as compared to Ag(111).[41] In particular, the induced charges and projected density of states (see Supporting Information, Figure S3) indicate that CHPR forms a stronger bond to Cu(111) than to Ag(111). Because the diffusion process of a surface-confined CHPR involves bond breaking and reforming, this difference in bond strength explains the trend in the diffusion barrier.

In a next step, we investigate covalent intermolecular bond formation between two CHPRs on Cu(111) and Ag(111). To do so, the proper definition of the starting configuration is crucial. The initial (II) state is shown in Figure 6 (left panels), where two CHPRs are anchored to atop sites and separated by two atomic rows of the metal substrate. After collecting several possible reaction pathways, we find that the system always passes through intermediate (IM) states in which the two CHPRs bind to a common surface metal atom. The final step of the reaction is given by covalent bond formation between the CHPRs. Note that in this final (FI) state the macrocycles of the CHP−CHP pair are both located on energetically favorable atop sites (Figure 6, right panels). The NEB calculations reveal that intermolecular CHPR coupling follows similar reaction pathways on Cu(111) and Ag(111), including diffusion steps toward IM states, and final covalent bond formation toward the (FI) state. However, inspection of the corresponding configurations and the energy diagrams of the reaction pathways depicted in Figure 6 reveals striking differences between the two substrates. These differences, as discussed in the following, are related to a radical-induced surface reconstruction and the matching of CHPR with respect to the metal surface lattice.

Along the path from II to FI, one radical performs a rotation around one unbroken CHPR−surface bond, while the other one is fixed to the surface atomic lattice. In our NEB procedure,

(41) Hammer, B.; Norskov, J. K. *Advances in Catalysis*; Academic Press Inc.: San Diego, CA, 2000; Vol. 45, pp 71−129.

only the initial (II) and final (FI) images are fixed, while all intermediate images are allowed to fully relax. This particular choice of II and FI states, in which one of the two molecules maintains its original atop site whereas the other one approaches, mimics a diffusing molecule encountering and eventually binding to an "immobilized" network cluster (which, in this case, is represented by a single molecule).

The initial step of the overall coupling process is determined by the diffusion of a "free" radical toward the first IM1 state (see the Supporting Information) and is activated by significantly different energies, notably 2.2 eV on Cu(111) and 0.8 eV on Ag(111). Further diffusion with small activation energies of 0.3 eV (Cu) and 0.1 eV (Ag) transfers the system toward the IM2 state. On Ag, the IM2 state is considerably more stable than the II state, where the two CHPRs are well separated. The energy difference between these two states can be explained by the rearrangement of atoms in the metal surface layer when the two CHPRs bind to a common surface atom (highlighted in orange in Figure 6): On Ag(111), this radical-induced surface reconstruction is significant, and an elevation of 1.7 Å is predicted for the central surface atom and of 0.7 Å for the other Ag atoms binding to the CHPRs. The significantly elevated central Ag atom is thus less coordinated to neighboring metal atoms, which eventually contributes to a stronger CHPR−Ag bond. On Cu(111), the geometry of the surface−CHPR complex is nearly unaffected upon the transition from the II to the IM2 state. Moreover, because of the calculated distance between CHPR hydrogen atoms of only 1.8 Å, intermolecular H···H repulsion results in a slightly higher energy of the IM2 (2.8 eV) as compared to the II state (2.5 eV).

The following two steps toward radical addition again reveal important differences on the two surfaces: On Cu(111), intermolecular bond formation is essentially barrierless and readily occurs from IM2 to IM3, which reflects a favorable configuration and intermolecular distance for bond formation (see insets of IM2 and IM3, where the orange sphere indicates the central atom binding to both CHPRs). However, inspection of the IM3 state shows that there is substantial stress on the CHP−CHP bond, and the system thus relaxes toward the favorable atop configuration in the FI state with an activation energy of 1.7 eV. On Ag(111), on the other hand, the configuration and intermolecular distance between the two CHPRs in the IM2 state are obviously less favorable for intermolecular coupling. During the transition from the IM2 to the IM3 state, one CHPR rotates about the central surface atom from the energetically favorable atop to a bridge site, which requires a significant amount of energy (1.8 eV). Eventually, bond formation and relaxation to atop sites in the FI state proceed readily with a barrier of 0.2 eV. The calculations thus strongly indicate that the difference between the two substrates with respect to 2D polymer formation is related to the favorable and less favorable matching of CHPR to the Cu and Ag surface lattice, respectively, as well as to the different chemical activities of Cu and Ag.

These findings have striking implications on the energy diagram of the overall reaction pathway. On Cu(111), the initial diffusion process (2.2 eV) is the rate-limiting step. Once this barrier is overcome, the reaction is predicted to proceed spontaneously because the path toward intermolecular bond formation (IM3 state) is essentially barrierless and the 1.7 eV required to relax the system is significantly lower than bond breaking (2.3 eV for IM3 to IM2) and backward diffusion (2.0 eV for IM2 to IM1). Thus, the surface-mediated polymerization on Cu with hindered diffusion and favored coupling corresponds ideally to the regime of diffusion-limited network formation, which explains why the branched clusters predicted by Monte Carlo simulations for this growth regime (Figure 5A) are in excellent agreement with experimental observations on Cu(111) (Figure 4A). Conversely, on Ag(111) the energy diagram shows that CHPR coupling is the rate-limiting step: Once the initial diffusion barrier of 0.8 eV is overcome, the system readily reaches the IM2 state, and backward diffusion with individual barriers of 0.9 (IM2 to IM1) and 0.8 eV (IM1 to II) is favored over covalent bond formation (1.8 eV), leading to an overall increased mobility of the molecules.

Here, a few more comments on the experimental conditions are required. The discussed formation of polyphenylene networks is obviously based on the self-assembly of molecules deposited on a surface. For metal aggregation processes, it was shown that the growth conditions and thus the morphology of the resulting clusters can be addressed by varying the deposition rate and substrate temperature. Thus, to have unbiased conditions, we used an identical and low deposition rate for all experiments reported here. Concerning temperature effects, we find no significant modifications of the network morphologies after performing the polymerization at different annealing temperatures. On the basis of the calculated energy diagram for CHPR/Cu(111), network growth is diffusion-limited and is thus not expected to change at higher temperatures. On the Ag surface, only at very high temperatures will the coupling probability increase. The barriers resulting from DFT reveal that diffusion-limited growth cannot be promoted by temperature.

A final important point in this discussion is the effect of coadsorbed iodine on the reaction mechanism. For verification, different sample preparation procedures were applied, in particular inducing the polymerization in a postannealing step or by immediately preparing the sample above the desorption temperature of iodine (not possible on Cu without the risk of surface degradation). Briefly, we find no evidence for iodine-induced network modification. This is consistent with previous findings on methyl radical coupling where the reaction pathways in the presence and absence of iodine remained unchanged.[42] These and our results thus suggest that the predominant effect of the halogen is to block surface sites and not to participate chemically in the coupling reaction. Collective electrostatic or indirect interaction effects mediated by the substrate might, however, contribute in reducing reaction barriers, which would require further theoretical investigation.

Conclusions

We investigated the adsorption and self-assembly of the hexaiodo-substituted macrocycle CHP on well-defined (111) surfaces of the coinage metals Cu, Au, and Ag. STM analysis shows that on either surface the adsorption of CHP follows a dissociative pathway with selective C−I bond cleavage, resulting in coadsorbed iodine and the evolution of surface-stabilized CHP radicals. Subsequent covalent intermolecular bond formation between CHP radicals toward covalently bonded polyphenylene networks is thermally activated by annealing the corresponding substrate to temperatures of about 475 K (Cu), 525 K (Au), and 575 K (Ag). The polymer networks show significantly different morphologies on the three substrates, ranging from branched, fractal-like structures

(42) Chiang, C. M.; Bent, B. E. *Surf. Sci.* **1992**, *279*, 79–88.
(43) Horcas, I.; Fernandez, R.; Gomez-Rodriguez, J. M.; Colchero, J.; Gomez-Herrero, J.; Baro, A. M. *Rev. Sci. Instrum.* **2007**, *78*, 8.
(44) Tersoff, J.; Hamann, D. R. *Phys. Rev. Lett.* **1983**, *50*, 1998–2001.

on Cu(111) to extended, regular 2D networks on Ag(111). DFT analysis of the diffusion and coupling pathways on Cu and Ag reveals that the balance between the diffusion and coupling steps is significantly different on the two substrates. On Cu, the radicals spontaneously form covalent intermolecular bonds once the initial diffusion barrier is overcome. Conversely, on the Ag surface, diffusion clearly prevails over intermolecular coupling, which results in an overall increased mobility of the radicals on the surface and in regular 2D network formation. With the aid of generic Monte Carlo simulations, we have shown that a high mobility (or low coupling affinity of the reactants) is a prerequisite for the growth of dense 2D polymer networks. However, the simulations also clearly indicate that even under favorable growth conditions defects in the network clusters have to be expected, demonstrating that surface-supported two-dimensional polymers based on irreversible reactions are inherently limited with respect to their structural perfection. Our results demonstrate that the substrate not only acts as a static support but that it is actively involved in all reaction steps and significantly influences the morphology of self-assembled covalently bonded nanostructures.

Acknowledgment. This work was supported by the Swiss National Science Foundation and the NCCR Nanoscale Science. Grants of beam time for XPS experiments at the Swiss Light Source (SLS), as well as extensive computing time at the Swiss National Supercomputing Center (CSCS), are gratefully acknowledged. We thank F. Nolting and the staff of the SIM beamline for experimental assistance, and H. Brune and S. Blankenburg for fruitful discussions.

Supporting Information Available: Experimental details, description of DFT calculation methods, considerations of the diffusion pathway and reaction mechanism of CHP on Cu(111) and Ag(111), and description of the Monte Carlo process for network growth simulations. This material is available free of charge via the Internet at http://pubs.acs.org.

JA107947Z